Acta Pharmaceutica Sinica B 2024;14(11):4776–4788

Chinese Pharmaceutical Association
Institute of Materia Medica, Chinese Academy of Medical Sciences

Acta Pharmaceutica Sinica B

www.elsevier.com/locate/apsb
www.sciencedirect.com

ORIGINAL ARTICLE

Activation of pregnane X receptor sensitizes alcoholic steatohepatitis by transactivating fatty acid binding protein 4

Yiwen Zhang[a,†], Bingfang Hu[a,†], Shaoxing Guan[a,†], Pan Li[h,†], Yingjie Guo[b], Pengfei Xu[c], Yongdong Niu[d], Yujin Li[a], Ye Feng[e], Jiewen Du[f], Jun Xu[f], Xiuchen Guan[g], Jingkai Gu[b], Haiyan Sun[i,*], Min Huang[a,*]

[a]*Institute of Clinical Pharmacology, School of Pharmaceutical Sciences, Sun Yat-sen University, Guangzhou 510006, China*
[b]*Research Center for Drug Metabolism, School of Life Sciences, Jilin University, Changchun 130015, China*
[c]*Department of Hepatobiliary and Pancreatic Surgery, Zhongnan Hospital of Wuhan University, School of Pharmaceutical Sciences, Wuhan University, Wuhan 430072, China*
[d]*Department of Pharmacology, Shantou University Medical College, Shantou 515031, China*
[e]*Department of Endocrinology and Metabolic Disease, the First Affiliated Hospital, Zhejiang University School of Medicine, Hangzhou 310003, China*
[f]*Research Center for Drug Discovery, School of Pharmaceutical Sciences, Sun Yat-sen University, Guangzhou 510006, China*
[g]*Department of Orthodontics, School of Stomatology, Capital Medical University, Beijing 100069, China*
[h]*Department of Electrical Engineering and Computer Science, Case School of Engineering, Case Western Reserve University, Cleveland, OH 44106, USA*
[i]*School of Food and Drug, Shenzhen Polytechnic University, Shenzhen 518055, China*

Received 29 March 2024; received in revised form 17 June 2024; accepted 25 July 2024

KEY WORDS

Alcoholic steatohepatitis;
Fatty acid binding protein 4;

Abstract Alcoholic steatohepatitis (ASH) is a liver disease characterized by steatosis, inflammation, and necrosis of the liver tissue as a result of excessive alcohol consumption. Pregnane X receptor (PXR) is a xenobiotic nuclear receptor best known for its function in the transcriptional regulation of drug metabolism and disposition. Clinical reports suggested that the antibiotic rifampicin, a potent human PXR

*Corresponding authors.
E-mail addresses: susan@szpu.edu.cn (Haiyan Sun), huangmin@mail.sysu.edu.cn (Min Huang).
[†]These authors made equal contributions to this work.

Peer review under the responsibility of Chinese Pharmaceutical Association and Institute of Materia Medica, Chinese Academy of Medical Sciences.

https://doi.org/10.1016/j.apsb.2024.08.029

Pregnane X receptor;
Alcoholic liver disease;
Andrographolide;
Nuclear receptor;
Liver injury;
Rifampicin

activator, is a contraindication in alcoholics, but the mechanism was unclear. In this study, we showed that the hepatic expression of fatty acid binding protein 4 (FABP4) was uniquely elevated in ASH patients and a mouse model of ASH. Pharmacological inhibiting FABP4 attenuated ASH in mice. Furthermore, treatment of mice with the mouse PXR agonist pregnenolon-16α-carbonitrile (PCN) induced the hepatic and circulating levels of FABP4 and exacerbated ASH in a PXR-dependent manner. Our mechanism study established FABP4 as a transcriptional target of PXR. Treatment with andrographolide, a natural compound and dual inhibitor of PXR and FABP4, alleviated mice from ASH. In summary, our results showed that the PXR−FABP4 gene regulatory axis plays an important role in the progression of ASH, which may have accounted for the contraindication of rifampicin in patients of alcoholic liver disease. Pharmacological inhibition of PXR and/or FABP4 may have its promise in the clinical management of ASH.

1. Introduction

Alcoholic liver disease (ALD) is defined as a liver pathology caused by excessive alcohol consumption and manifested by simple steatosis, steatohepatitis, liver fibrosis, or cirrhosis[1,2]. ALD is increasingly becoming a major form of liver disease worldwide[3]. In the clinic, alcoholic steatohepatitis (ASH) is commonly characterized by concurrent steatosis, inflammation, and necrosis of the liver tissue. Some ASH will eventually progress to hepatocellular carcinoma (HCC)[4]. According to the latest epidemiological analysis in the United States, 32%−45% of HCC are triggered by chronic alcohol over-intake[5]. The proposed mechanisms for alcohol-induced liver injury include oxidative stress, lipid peroxidation, acetaldehyde toxicity, and secretion of pro-inflammatory cytokines[6-8]. However, many of these proposed mechanisms have their limitations in explaining the pathogenesis of ALD. Largely due to the lack of sufficient understanding of alcohol-induced liver injury, there are no specific drugs in the clinic to treat ALD or ASH. Rather, the most frequently used interventions are alcohol abstinence and symptom management[2].

The fatty acid binding protein 4 (FABP4, or aP2) is a lipid transporter best known for its expression and function in the adipocytes and macrophages[9]. FABP4 can also be secreted into the circulation, and it is expressed by many other tissues, including the liver. Both animal and clinical studies have suggested a pro-inflammatory and pathogenic effect of FABP4. Elevated tissue expression and/or circulating levels of FABP4 have been correlated with a battery of local and systemic diseases[10], such as non-alcoholic steatohepatitis[11], obesity[12], type II diabetes[13], insulin resistance, atherosclerosis[14], osteoporosis[15], and oncogenesis[16]. As a transcriptional target of PPARγ, LXRα and AP-1[17], FABP4 plays a major role in macrophage infiltration and tissue injuries[18]. We have previously reported that overexpression of FABP4 sensitized mice to ischemia/reperfusion-induced liver injury, and FABP4 is a transcriptional target of the hypoxia inducible factor-1 alpha[19]. We also reported that FABP4 played a pathogenic role in sepsis, and pharmacological inhibition of FABP4 attenuated mice from sepsis-induced hepatic and pulmonary injuries[20]. However, the role of FABP4 in the pathogenesis of ALD and ASH remains to be clearly defined.

Pregnane X receptor (PXR, NR1I2) is a nuclear receptor best known for its function as a master regulator of xenobiotic and endobiotic metabolism[21,22]. PXR is predominantly expressed in the liver and intestine. Subsequent studies also suggested a regulatory effect of PXR on cholesterol and lipid homeostasis[23]. Ablation of PXR and activation of PXR alleviated mice from and sensitized mice to diet-induced obesity and insulin resistance, respectively[24]. PXR has also been shown to play an important role in the pathogenesis of non-alcoholic steatohepatitis by increasing the expression of genes involved in lipid uptake and synthesis, such as Lipin 1, CD36, and SCD1[25,26]. A recent report suggested that chronic alcohol exposure enhanced the nuclear translocation of mouse PXR and induced the expression of PXR target genes in the liver[27]. However, the pathophysiological significance of this observation has not been thoroughly investigated. On the other hand, Rifampicin (RIF), an antibiotic and potent human PXR agonist, is a clinical contraindication that can aggravate liver injuries in alcoholics[28]. A recent study reported a protective effect of PXR ablation in a mouse model of ALD, but the mechanism is yet to be defined[29].

Andrographolide (AG) is the major active ingredient of the herbal plant *Andrographis Paniculata*, which has been widely used in Asian countries for the treatment of sepsis, hypertension, scald, and venomous snake bites[30]. Recent studies have suggested that AG has many therapeutic effects, ranging from anti-bacterial to anti-inflammatory, anti-tumorigenesis, hepatoprotective, and improving cardiovascular functions[31,32]. Pretreatment with AG also attenuated mice from chemical-induced liver injury[33]. Molecular-docking and *in vitro* studies suggested AG as a dual inhibitor of FABP4[34] and PXR[35]. However, whether and how AG may have a protective effect on ASH is unknown.

In this study, we uncovered novel functions of PXR and FABP4 in ASH. Pharmacological inhibition of FABP4 protected mice from ASH. Activation of PXR sensitized mice to ethanol-induced hepatic injury by inducing *FABP4*, a PXR target gene. In contrast, pharmacological inhibition of the PXR−FABP4 gene regulatory axis by AG alleviated mice from ASH. Our results suggest the PXR−FABP4 axis as a novel therapeutic target, and AG as a potential drug for the treatment of alcoholic steatohepatitis.

2. Materials and methods

2.1. Bioinformatic analysis of the gene expression omnibus (GEO) datasets

The mRNA expression of *FABP4* in clinical samples was analyzed in relevant datasets from the GEO database (http://www.ncbi.nlm.nij.gov/geo). In briefly, the hepatic FABP4 expression profile of alcoholic hepatitis patients were derived from GSE28619, and this transcriptional change was further confirmed in GSE143318. The

pattern of FABP4 expression changes in patients with various stages of alcoholic liver diseases was derived from GSE103580. The PCN effect on the hepatic *FABP4* gene expression was derived from GSE123804. The hepatic gene expression patterns of NR1I2/PXR and CYP3A11 in mice with prolonged ethanol diet were derived from GSE86002.

2.2. Animals, drug treatments, and experimental designs

C57BL/6J male mice were purchased from the Guangzhou University of Chinese Medicine (Guangzhou, China). Mice were challenged with the NIAAA model of ASH[36]. In brief, mice were initially fed with control Lieber-DeCarli diet *ad libitum* for 5 days. Afterwards, alcohol groups were allowed free access to ethanol Lieber-DeCarli diet containing 5% (*v*/*v*) ethanol for 10 days, and control groups were pair-fed with the isocaloric control diet. The body weight was measured during the ethanol feeding. On Day 11, alcohol and pair-fed groups were gavaged with a single dose of ethanol (5 g/kg) or isocaloric maltose dextrin, respectively. Mice were then euthanized, and the tissues were collected 9 h later. When necessary, mice received a daily treatment of drugs along with the ethanol diet before tissue harvesting. PCN (80 mg/kg), BMS309403 (20 mg/kg), or quercetin (100 mg/kg) were given by gavage, and andrographolide (50 mg/kg) was administrated by intraperitoneal injections. The Alb-VP-PXR and FABP-VP-PXR transgenic mice were previously described[24,37], and have been backcrossed to the C57BL/6J background for at least eight generations. For the acute alcohol consumption model, mice were given acute treatment of ethanol by gavage every 12 h (4.5 g/kg, for a total of three times). Samples were then collected 6 h after the last dose[38]. For the alcohol-induced liver fibrosis model, mice were first fed with high-fat Lieber-DeCarli diet for adaptation. The disease group was then exposed to the same diet supplemented with 2% ethanol for 17 days, and carbon tetrachloride (CCl_4) was i.p. injected twice per week at the dosage of 1 μL/g (Days 4, 7, 11 and 14)[39]. The use of mice in this study has complied with relevant guidelines and institutional policies. This study was approved by the Institutional Animal Care and Use Committee of Sun Yat-sen University (Guangzhou, China).

2.3. Real-time PCR analysis, Western blotting, and enzyme-linked immunosorbent assay (ELISA)

For gene expression analysis, liver total RNA was extracted with TRIzol reagent from Thermo Fisher (Carlsbad, CA, USA). Reverse transcription was performed with random hexamer primers and Superscript RT III enzyme. The cDNA was then detected with the SYBR Green real-time PCR kit by using the ABI 7300 system from Applied Biosystems (Foster City, CA)[40]. Data were normalized against the house-keeping gene GAPDH. Sequences of the real-time PCR primers are listed in Supporting Information Table S1. To measure hepatic FABP4 protein levels, tissues were homogenized, and total protein was prepared with lysis buffer. Western blotting was then performed as previously described[24]. The FABP4 antibody (D25B3, Cat #3544) was purchased from Cell Signaling (Danvers, MA, USA). GAPDH antibody (sc-25778, Cat #D3015) was purchased from Santa Cruz (Dallas, TX, USA). For the quantification of circulating levels of FABP4, a mouse FABP4 ELISA kit was purchased from Biological Immune Method (San Francisco, CA, USA), and the experiment was performed according to the manufacturer's instructions.

2.4. Serum and liver biochemistry

The serum levels of total triglyceride (TG), aspartate transaminase (AST), and alanine transaminase (ALT) were measured with commercial assay kits. For the measurement of hepatic lipid levels, tissues were homogenized, and total triglycerides were extracted with chloroform/methanol solution. The TG levels were measured and normalized against tissue protein concentrations.

2.5. Tissue histology

Tissues were fixed in 4% formaldehyde and embedded in paraffin. The paraffin blocks were then sectioned at 5 μm and stained with hematoxylin and eosin (H&E) for general histology. Frozen liver tissues were sectioned at 8 μm and used for Oil-red O staining. To quantify liver lipid droplets, digital images of Oil-red O sections were analyzed by Image-Pro Plus 6.0 software from Media Cybernetics (Rockville, MD, USA).

2.6. Plasmid construction, transient transfection, and reporter gene assay

The mouse *Fabp4* gene promoter sequences were PCR-amplified by using mouse liver genomic DNA as the template. The primer sequences are listed in Table S1. Both amplified fragments and pGL3-basic vector (Promega, Madison, WI, USA) were digested with KpnI and XhoI before ligation using the T4 DNA ligase. The cloned promoter sequences were verified by DNA sequencing. For transient transfection and luciferase reporter gene assay, CV-1 cells were cultured in Eagle's minimum essential medium supplemented with 10% fetal bovine serum and transfected in 48-well plates by using Lipofectamine 3000 reagent from Thermo Fisher. The transfected cells were cultured for an additional 48 h with or without 10 nmol/L PCN before luciferase assay. The luciferase value was normalized against β-gal activity derived from the co-transfected pCMX-β-gal plasmid.

2.7. Electrophoretic mobility shift assay

Briefly, the ^{32}P-labeled oligonucleotides were incubated with PXR and RXR proteins *in vitro* synthesized by a TNT kit from Promega. The DNA−protein complexes in reaction buffer were then separated by electrophoresis for 3 h. Both unlabeled wild-type and mutant oligonucleotides were included for competition experiments. The EMSA probe sequences are listed in Table S1.

2.8. Molecular docking analysis

Based on a previous report[41], we performed docking analyses to further investigate the mode of interaction between AG and either PXR or FABP4. In brief, the Protein Data Bank format of PXR (4 × 1F) and FABP4 (5HZ6) were downloaded from the RCSB Protein Data Bank (http://www.rcsb.org/). The docking analysis was conducted by using Molecular Operating Environment software from Chemical Computing Group (Montreal, Canada). We focused on two parameters: the docking score, which represents the energy of interaction between protein and inhibitor, and the hydrogen bond interactions between receptor residues and chemical. The docking results were then compared with "positive controls," such as the PXR−ketoconazole, FABP4−BMS309403 and GSK3β−AG complexes, whose docking scores were calculated by the same software[41].

2.9. Statistics

In the bioinformatic analysis, genes with top differentially regulated expression levels were filtered by the GEO2R online platform. If one probe set does not contain the homologous gene, the data is removed. If one gene has numerous probe sets, the result will be further investigated with SangerBox software (http://sangerbox.com/). The calculated DEGs (differentially expressed genes) are presented as heatmaps and volcano plots. The protein−protein interaction (PPI) network of identified DEGs was constructed by using STRING database (https://string-db.org/). In the experimental studies, all analysis was carried out with the Statistical Package for Social Sciences (SPSS) software version 16.0. Data are expressed as mean ± standard deviation (SD), and the statistical significance between two individual groups was determined by the Student *t*-test. Differences among multiple groups were evaluated by using one-way analysis. A *P* value of less than 0.05 was considered as significantly different.

3. Results

3.1. The expression of FABP4 is elevated in patients of alcoholic hepatitis

To evaluate the correlation between FABP4 levels and alcohol-triggered liver injuries, we analyzed DEGs from the GEO dataset GSE28619 derived from the livers of patients of alcoholic hepatitis and their normal controls. A significant increase of hepatic *FABP4* gene expression was found in alcoholic hepatitis patients as shown by heatmap (Fig. 1A), volcano plot (Fig. 1B), and relative gene expression (Fig. 1C). We then used the Search Tool for the Retrieval of Interacting Genes/Proteins (STRING) platform[42] to construct a PPI network among DEGs. As shown in Fig. 1D, our enrichment analysis indicated strong connections between FABP4 and some major genes involved liver steatosis and inflammation, which inspired us to explore the pathological role of FABP4 in the progress of alcoholic steatohepatitis, because both steatosis and inflammation are hallmarks of alcoholic steatohepatitis. An increased hepatic expression of FABP4 (Supporting Information Fig. S1A) and a similar pattern of DEG PPI (Fig. S1B) were observed in another independent dataset GSE143318, in which the hepatic expression of FABP4 was elevated by approximately 15-fold in patients of severe alcoholic hepatitis compared to their healthy controls. Similar results were also observed in transcriptome datasets GSE167308, GSE100901 and GSE142530, respectively (Fig. S1C). To further understand the dynamics of hepatic FABP4 expression in various stages of alcoholic liver diseases, we analyzed the stage-specific expression of FABP4 in GSE103580. As shown in Fig. 1E, the hepatic mRNA expression of *FABP4* in alcoholic hepatitis or alcoholic cirrhosis patients was higher than their alcoholic simple steatosis counterparts.

3.2. The expression of FABP4 is induced in mouse model of alcoholic steatohepatitis

To examine the *in vivo* relevance of FABP4 expression and induction in ALD, we established several mouse models of ALD, including acute alcohol exposure (alcoholic fatty liver) in which mice were gavaged with high doses of ethanol[38], alcoholic liver fibrosis in which mice were treated with high-fat Lieber- DeCarli diet together with the treatment of CCl_4 to induce fibrosis[39], as well as the NIAAA model of alcoholic steatohepatitis in which mice were treated with ethanol liquid diet for 10 days before acute ethanol gavage[36], as outlined in Supporting Information Fig. S2. Upon acute alcohol exposure, mice suffered from weight loss and hepatomegaly (Fig. 2A). Histological analysis showed a balloon-like lesion and increased lipid accumulation (Fig. 2B). However, despite signs of tissue injury, the serum levels of AST and ALT were not affected (Fig. 2C), whereas the hepatic mRNA expression of *IL6* was markedly suppressed (Fig. 2D). Interestingly, although the hepatic mRNA expression of *FABP4* showed a trend of increase, the hepatic protein expression of FABP4 was decreased in the acute alcohol exposure group (Fig. 2E). A similar pattern of phenotype was observed in the mouse model of alcoholic liver fibrosis (Fig. 2F−J).

In contrast, the NIAAA model of alcoholic steatohepatitis exhibited more clinically relevant ALD features. These include unchanged body weight along with hepatomegaly (Fig. 2K), marked steatosis (Fig. 2L), increased serum levels of AST and ALT (Fig. 2M), increased hepatic expression of IL6 (Fig. 2N), and increased expression of FABP4 at both the mRNA and protein levels (Fig. 2O). The stage-specific effects of ALD on the expression of FABP4 was consistent with those observed in ALD patients (Fig. 1E). Since the NIAAA mouse model of alcoholic steatohepatitis better recapitulated the human ASH, we will focus on using this model for our remaining studies.

3.3. Pharmacological inhibition of FABP4 attenuates mouse model of alcoholic steatohepatitis

To determine the functional relevance of ASH responsive induction of FABP4, we examined the effect of the synthetic FABP4 inhibitor BMS309403[13] and the natural product FABP4 inhibitor quercetin[34] on the NIAAA model of ASH. In this experiment, male mice were gavaged with 20 mg/kg BMS309403, 100 mg/kg quercetin, or vehicle along with the ethanol diet. As shown in Fig. 3A, administration with either BMS309403 or quercetin led to attenuation of alcohol-induced hepatomegaly without affecting the total body weight. Necropsy and histological analysis revealed that BMS309403- or quercetin-treated mice showed improved gross appearance of the liver, as well as reduced balloon-like lesions and lipid accumulation (Fig. 3B). Quantification of the Oil Red-O staining showed a decreased distribution of larger lipid droplets in both BMS309403- and Quercetin-treated groups (Fig. 3C). At the biochemical level, the ASH responsive inductions of serum AST and ALT were ameliorated under the quercetin treatment (Fig. 3D). Moreover, levels of serum and liver triglyceride were attenuated by the treatment of both inhibitors (Fig. 3E). Consistent with the improved histology, the hepatic expression of IL-6 was also inhibited in the two inhibitor groups (Fig. 3F).

3.4. Pharmacological activation of PXR induces FABP4 and sensitizes mice to alcoholic steatohepatitis, which can be attenuated by a FABP4 inhibitor

Knowing RIF, a human PXR agonist, is a contraindication of ALD in the clinic, we speculated that RIF may have aggravated ALD by activating PXR. To test this hypothesis, WT mice were subjected to the ASH model in the absence or presence of oral gavage of the mouse PXR agonist PCN (80 mg/kg). Treatment with PCN exacerbated hepatomegaly (Fig. 4A) and steatosis (Fig. 4B), along

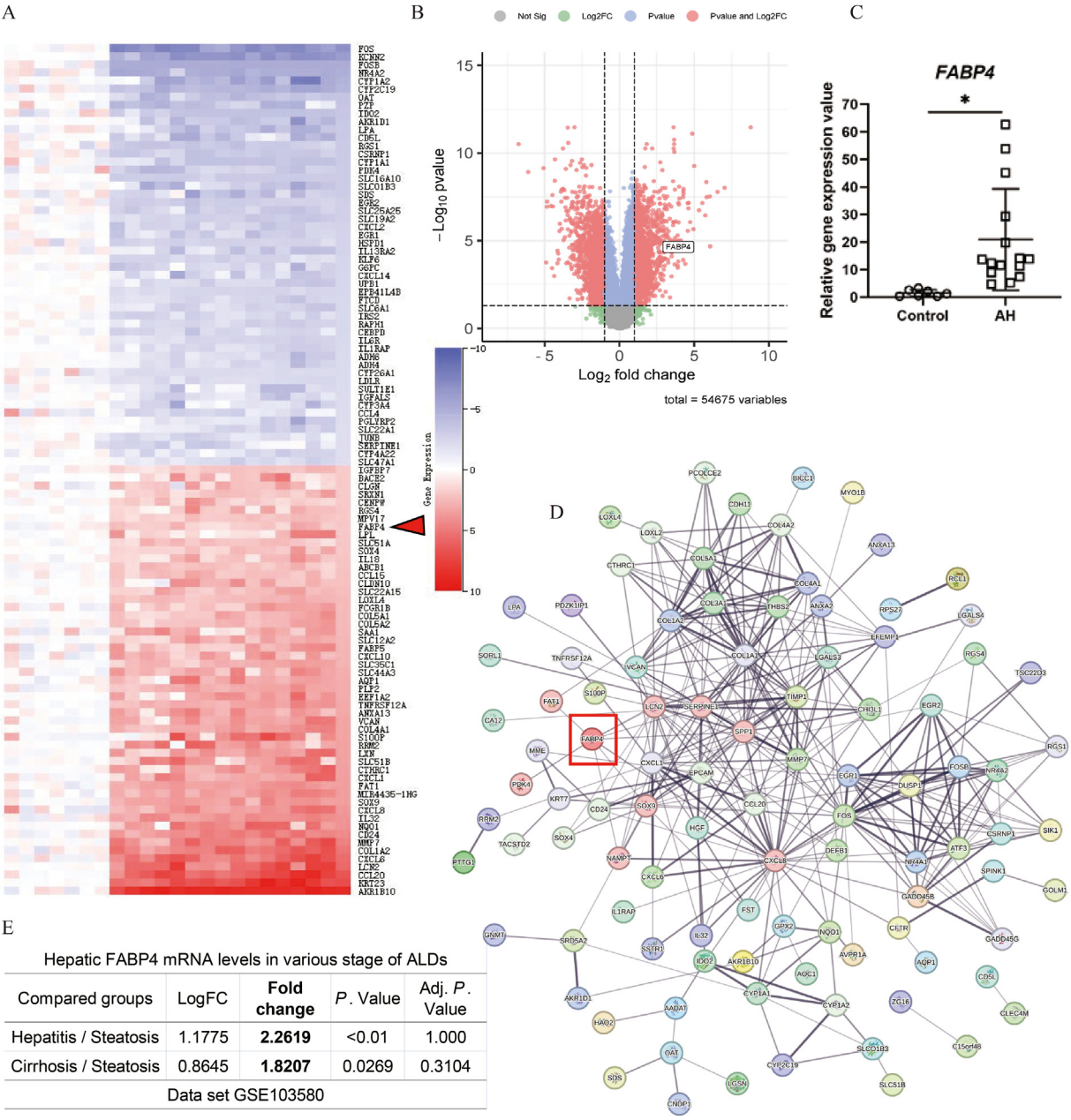

E

Hepatic FABP4 mRNA levels in various stage of ALDs

Compared groups	LogFC	**Fold change**	*P*. Value	Adj. *P*. Value
Hepatitis / Steatosis	1.1775	**2.2619**	<0.01	1.000
Cirrhosis / Steatosis	0.8645	**1.8207**	0.0269	0.3104
Data set GSE103580				

Figure 1 The expression of FABP4 is elevated in patients of alcoholic hepatitis. The top regulated genes during alcoholic hepatitis are shown in heatmap (A) and volcano plot (B). (C) The hepatic levels of *FABP4* mRNA in healthy control subjects and patients with alcoholic hepatitis. The open circles and squares represent individual patients. (D) The protein−protein interaction network of top differently expressed genes in alcoholic hepatitis. The analysis was performed on transcriptome dataset GSE28619. (E) The gene expression level of *FABP4* in various stage of alcoholic liver disease. The analysis was performed on transcriptome dataset GSE103580. Data are presented as mean ± SD, ***$P < 0.001$.

with an increased percentage of larger lipid droplets (Fig. 4C), AST (Fig. 4D), serum and liver triglyceride levels (Fig. 4E), and IL6 expression (Fig. 4F). The exacerbation of ASH by PCN was accompanied by the induction of hepatic mRNA expression of *FABP4* (Fig. 4G), as well as the serum level of FABP4 (Fig. 4H). To determine whether the induction of FABP4 was relevant in the sensitizing effect of PCN, we co-treated mice with the FABP4 inhibitor quercetin. Co-treatment with quercetin largely abrogated the Pro-ASH effect of PCN (Fig. 4A−H), suggesting that the induction of FABP4 was at least partly responsible for the ASH sensitizing effect of PCN. We also showed that the sensitizing effect of PCN was PXR dependent because treatment of PXR knockout mice[43] subjected to the ASH model with PCN had little effect on the serum levels of AST and ALT (Fig. 4I). PCN no longer induced the expression of FABP4 in PXR null mice (Fig. 4J).

PXR is also known to induce the expression of other hepatic genes involved in lipid uptake, including the fatty acid uptake transporter *Cd36*[23]. We found that although the hepatic mRNA expression of *Cd36* was induced by ASH, the expression of *Cd36* was not significantly affected by PCN treatment in the ASH model (Supporting Information Fig. S3A). Furthermore, our

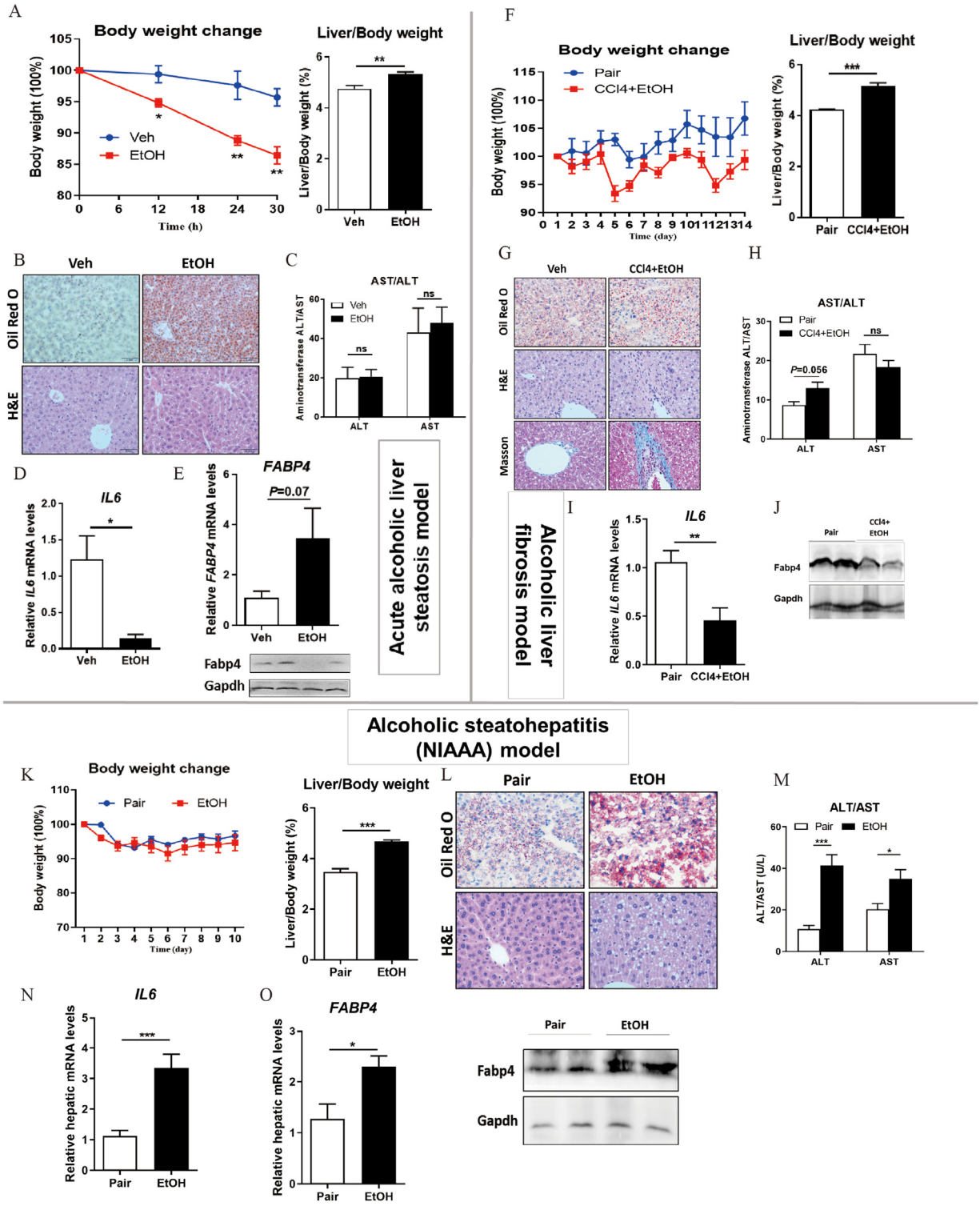

Figure 2 The expression of FABP4 is induced in mouse model of alcoholic steatohepatitis. (A−E) C57BL/6 male mice were subjected to the acute alcohol exposure model. Shown are growth curve and liver/body weight ratio of acute alcohol exposure model (A), histological analysis of liver samples (scale bar: 50 μm) (B), serum AST and ALT levels (C), and the hepatic levels of IL6 (D) and FABP4 (E). (F−J) C57BL/6 male mice were subjected to alcoholic liver fibrosis model. Shown are growth curve and liver/body weight ratio of mice (F), histological analysis of liver samples [scale bar: 50 μm] (G), serum AST and ALT levels (H), and the hepatic levels of IL6 (I) and FABP4 (J). (K−O) C57BL/6 male mice were subjected to NIAAA model of alcoholic steatohepatitis. Shown are growth curve and liver/body weight ratio of mice (K), histological analysis of liver samples (scale bar: 50 μm) (L), serum AST and ALT levels (M), and the hepatic mRNA expression of IL6 (N) and hepatic mRNA and protein levels of FABP4 (O). Data are presented as mean ± SD, $n = 4–6$; $^{*}P < 0.05$, $^{**}P < 0.01$, $^{***}P < 0.001$. ns, statistically not significant.

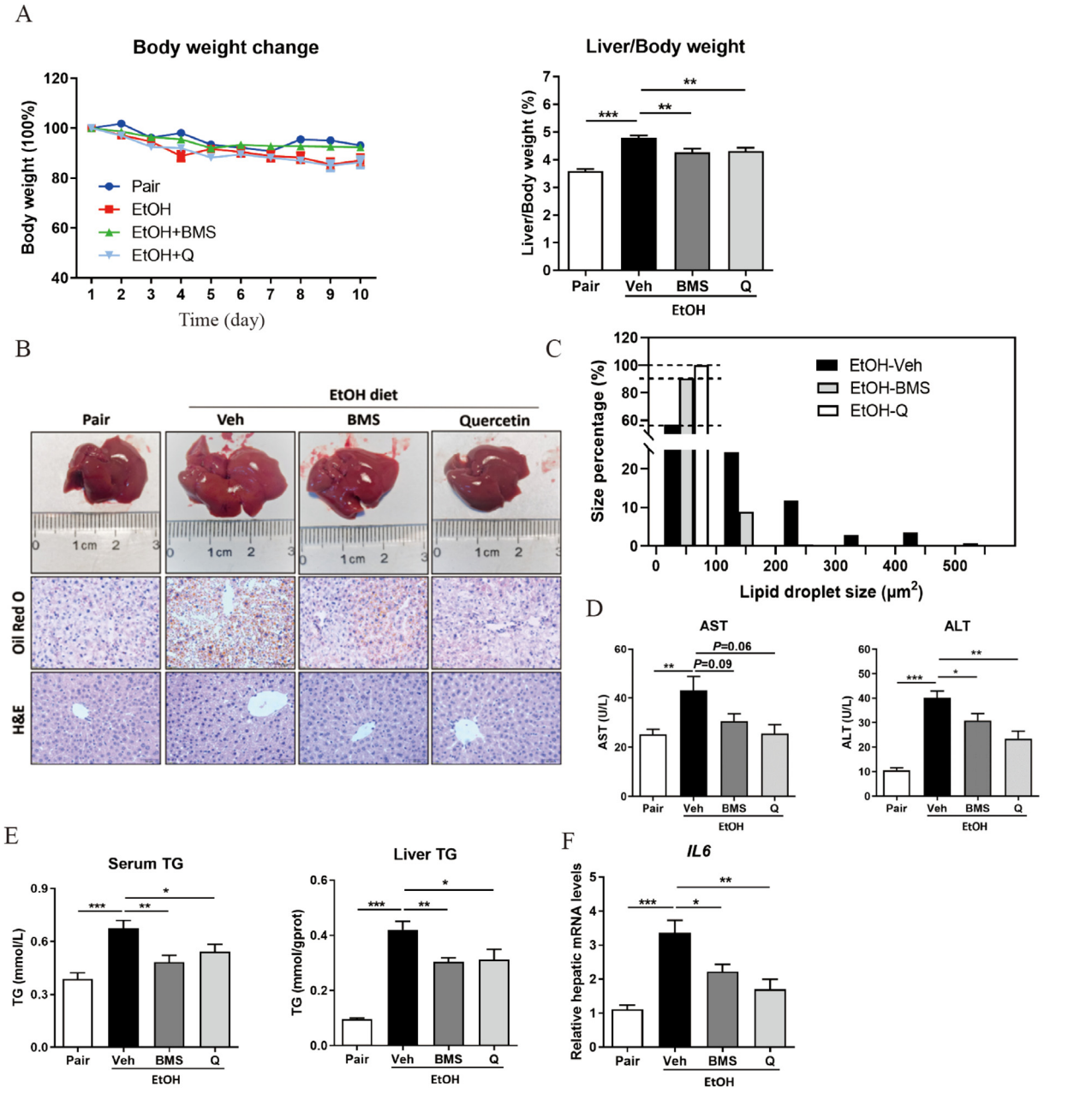

Figure 3 Pharmacological inhibition of FABP4 attenuates mouse model of alcoholic steatohepatitis. C57BL/6 male mice were subjected to NIAAA model of alcoholic steatohepatitis in the presence of vehicle, BMS309403 (25 mg/kg), quercetin (100 mg/kg) given daily by gavage. (A) Growth curve and liver/body weight ratio of mice. (B) Histological analysis of liver samples (scale bar: 50 μm). (C) Distribution of lipid droplet sizes in liver sections. (D) Serum AST and ALT levels. (E) Serum and hepatic TG levels. (F) The hepatic mRNA levels of *IL6*. Data are presented as mean ± SD, $n = 5-6$; *$P < 0.05$, **$P < 0.01$, ***$P < 0.001$.

bioinformatic analysis of GSE28619 dataset showed the expression of CD36, ACC1, FAS, and SCD was not affected in ASH patients (Fig. S3B). These results suggested that the regulation of Cd36 or other lipogenic genes may not be involved in the sensitizing effect of PXR activation on ASH.

3.5. *FABP4 is a transcriptional target of PXR*

We used transgenic mice bearing constitutive activation of PXR in the liver (Alb-VP-PXR) or both the liver and intestine (FABP-VP-PXR)[24,37] to further validate the induction of FABP4 by PXR activation. VP-PXR was constructed by fusing the VP16 activation domain to the N-terminus of the human PXR cDNA. Consistent with the induction of FABP4 in PCN-treated mice, the expression of FABP4 was markedly induced in both transgenic lines, along with the expected induction of the known PXR target gene *CYP3A11* (Fig. 5A). Consistent with our observation that PCN no longer induced the expression of FABP4 in PXR null mice (Fig. 4J), bioinformatics analysis of GSE123804 revealed that the hepatic expression of FABP4 and CYP3A11was

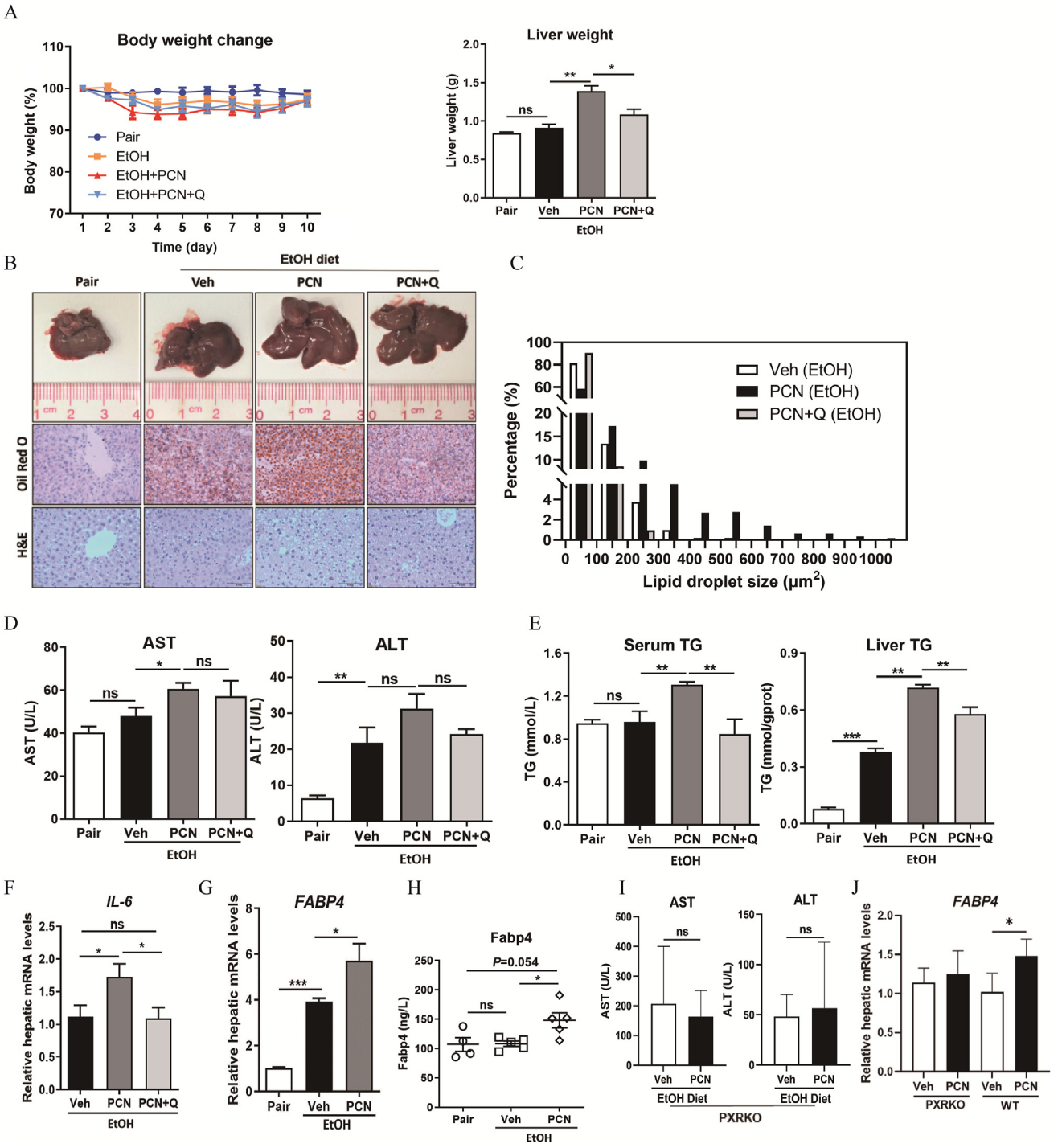

Figure 4 Pharmacological activation of PXR induces FABP4 and sensitizes mice to alcoholic steatohepatitis, which can be attenuated by a FABP4 inhibitor. (A−H) WT C57BL/6 male mice were subjected to NIAAA model of alcoholic steatohepatitis in the presence of vehicle, PCN (80 mg/kg), or PCN (80 mg/kg) + quercetin (100 mg/kg) given daily. Shown are growth curve and liver weight and liver/body weight ratio of mice (A), histological analysis of liver samples (scale bar: 50 μm) (B), distribution of lipid droplet sizes in liver sections (C), serum AST and ALT levels (D), serum and hepatic TG levels (E), the hepatic mRNA levels of IL6 (F), the hepatic mRNA levels of FABP4 (G), and serum levels of FABP4 protein (H). (I, J) Male PXRKO mice were subjected to NIAAA model of alcoholic steatohepatitis in the presence of vehicle or PCN (80 mg/kg). Shown are serum AST and ALT levels (I) and the hepatic mRNA levels of FABP4 (J). Data are presented as mean ± SD, $n = 5-6$; $^{*}P < 0.05$, $^{**}P < 0.01$, $^{***}P < 0.001$. ns, statistically not significant.

unchanged upon PCN treatment in PXR knockout mice (Fig. 5B). Interestingly, the PCN induction of FABP4 in WT mice was not observed in the ileum (Fig. 5B), suggesting the induction was liver specific. These results strongly suggested that the mouse *FABP4* is a PXR target gene.

To directly test whether *FABP4* is a PXR target gene, we constructed a luciferase reporter gene containing 500-bp of the mouse *FABP4* gene promoter and examined its regulation by PXR in a transient transfection and reporter gene assay. As shown in Fig. 5C, in CV-1 cells co-transfected with the reporter and the mouse PXR expression vector, treatment with PCN (10 nmol/L) induced the reporter activity to approximately 3-fold. The activation of the PXR responsive tk-CYP3A23-Luc reporter gene, which contains the PXR response element from the rat *CYP3A23* gene promoter[40], was included as a positive control. Our bioinformatic inspection of the mouse *FABP4* gene promoter revealed a direct repeat spaced by three nucleotides (DR3) type of PXR response element (PXRE) near the transcriptional starting site (Fig. 5D). The binding of PXR−RXR heterodimers to this PXRE was confirmed by electrophoretic mobility shift assay (EMSA) using radiolabeled PXRE and *in vitro* synthesized PXR and RXR proteins. As shown in Fig. 5E, the PXR−RXR heterodimers bound to PXRE, and the binding was efficiently competed by unlabeled PXRE, but not its mutant variant. The PXRE from the *CYP3A23* gene promoter was included as a positive control (Fig. 5E). In addition, our bioinformatic analysis of the publicly available ChIP-Seq data derived from PCN-treated mouse liver[44] revealed multiple PXR binding peaks around the distal region of mouse FABP4 gene (Supporting Information Table S2). However, future studies are necessary to pinpoint the PXR binding motifs within these binging peaks.

3.6. *The PXR and FABP4 dual inhibitor andrographolide protects mice from alcoholic steatohepatitis*

Having established the role of PXR−FABP4 gene regulatory axis in exacerbating alcoholic steatohepatitis, it is conceivable that drugs that block this axis may have therapeutic potentials.

A

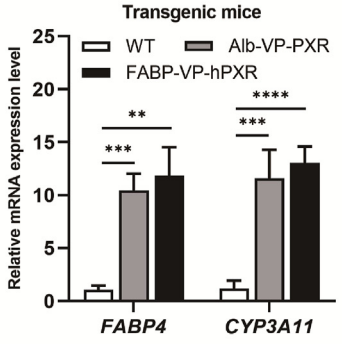

B

PCN (100 mg/kg) *vs* Control

Data set GSE123804

Gene	Tissue	Genotype	Log2 (FC)	FC	*P* Value	Adj. *P* Value
FABP4	Liver	**WT**	**0.95**	**1.93**	**<0.01**	**0.01**
		PXRKO	0.13	1.1	ns	ns
	Ileum	WT	0.17	1.13	ns	ns
		PXRKO	0.65	1.57	0.01	ns
CYP3A11	Liver	**WT**	**3.64**	**12.48**	**<0.01**	**<0.01**
		PXRKO	0.36	1.28	ns	ns
	Ileum	**WT**	**3.49**	**11.27**	**<0.01**	**<0.01**
		PXRKO	-0.05	0.97	ns	ns

C

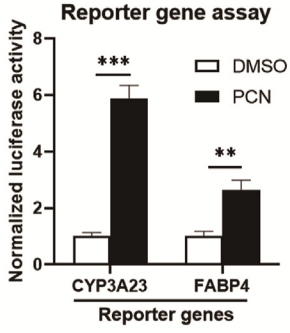

D

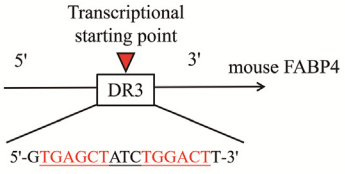

E

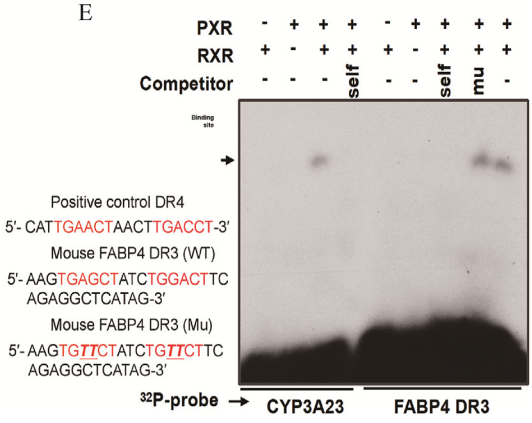

Figure 5 FABP4 is a transcriptional target of PXR. (A) Hepatic mRNA expression of *FABP4* and *CYP3A11* in WT, Alb-VP-PXR and FABP-VP-hPXR transgenic mice. (B) Hepatic mRNA expression of *FABP4* and *CYP3A11* in the liver and ileum of mice treated with the vehicle control or PCN. The analysis was performed on the liver transcriptome dataset GSE123804 from the GEO2R. (C) Mouse *FABP4* promoter reporter gene was transfected into CV-1 cells together with the expression vector for PXR. The transfection efficiency was normalized against the β-gal activity from the co-transfected CMX-β-gal vector. The PXR responsive CYP3A23 reporter was included as a positive control. Normalized luciferase activity of each type of reporter in cells treated with DMSO was arbitrarily set as 1. (D) Putative DR3-type PXR binding sites in the mouse *FABP4* gene promoter. (E) The binding of PXR−RXR heterodimers to ^{32}P-labeled FABP4 DR3 was demonstrated by electrophoretic mobility shift assay (EMSA). The sequences of wildtype (WT) DR3 and its mutant variant (Mu) are shown on the left. The binding of a known DR4-type PXRE by PXR−RXR heterodimers was included as positive controls. Data are presented as mean ± SD, $n = 10-12$; $^{*}P < 0.05$, $^{**}P < 0.01$, $^{***}P < 0.001$.

Published molecular docking and *in vitro* studies suggested AG as a dual inhibitor of FABP4[34] and PXR[35], and these notions were further supported by our own molecular docking analyses as shown in Fig. 6A and with the interactions between ligands and receptor pockets labeled as dashed lines. The energy scores of AG binding towards FABP and PXR pockets were −8.46 kcal/mol and −9.15 kcal/mol, respectively, which are considered stable interactions and comparable to those of the FABP4−BMS309403 (−11.2 kcal/mol) and PXR−ketoconazole (KTZ) (−9.1 kcal/mol) complexes.

To test the anti-ASH effect of AG *in vivo*, mice were daily i.p. injected with AG (50 mg/kg) while the mice were subjected to the 11-day ASH regimen. Treatment with AG attenuated hepatomegaly (Fig. 6B) and steatosis (Fig. 6C), decreased the percentage of larger lipid droplets (Fig. 6D), lowered the serum levels of AST and ALT (Fig. 6E) and serum and liver levels of triglycerides (Fig. 6F). Interestingly, treatment with AG also modestly decreased the animal's body weight (Fig. 6B), which was likely accounted for by decreased white adipose tissue mass and adipocyte sizes (Supporting Information Fig. S4), but the mechanism remains to be defined. Future experiments are necessary to determine whether lower and/or less frequent doses of AG are sufficient to provide the same protection without causing the decrease of body weight. Treatment with AG had little effect on food intake, which was consistent with a report that AG reduced body weight of HFD-fed mice without affecting food intake[45]. Fig. 6G summarizes our proposed role of the PXR-FABP4 regulatory axis in ASH.

4. Discussion

In this study, we reported the ASH sensitizing effect of the PXR−FABP4 regulatory axis. Hepatic induction of FABP4 was found in both ASH patients and the mouse model of ASH. Pharmacological inhibition of FABP4 alleviated mice from ASH. In contrast, activation of PXR by PCN induced the hepatic expression of FABP4 and exacerbated ASH pathology. The sensitizing effect of PCN was attenuated by the co-treatment of the FABP4 inhibitor quercetin. The mouse *FABP4* gene was established as a transcriptional target of PXR. Based on these results, we then identified Andrographolide as a natural compound that has a dual antagonizing effect towards PXR and FABP4 and verified its therapeutic effect against ASH.

Although elevated expression of FABP4 has been shown to contribute to the pathogenesis of obesity, type II diabetes, carcinogenesis, and atherosclerosis due to the activation of FABP4 in adipocytes and macrophages, the role of FABP4 in alcoholic steatohepatitis has not been reported. The current study has expanded the function of FABP4 to the liver and in the context of ALD. The role of FABP4 in ALD is intriguing. Our results suggested that the hepatic FABP4 was uniquely elevated in ASH, whereas the hepatic protein levels of FABP4 were decreased in acute ethanol exposure and alcoholic fibrosis. To understand this inconsistency, we found that there were dramatic morphological changes in the white adipose tissue (WAT) in mice challenged with the acute alcohol exposure and CCl_4/fibrosis models (Supporting Information Fig. S5). Since WAT is a major tissue produces and secrets FABP4, the alterations in WAT can potentially influence the circulating and hepatic levels of FABP4.

The stage-specific effects of ALD on the expression of FABP4 in mice were consistent with the observations from clinical samples, as the hepatic mRNA levels of FABP4 was higher in alcoholic hepatitis patients than in alcoholic simple steatosis patients. The mechanism for the stage specific effect of ALD on the expression of FABP4 remains to be defined. In the liver, hepatocytes are likely the major source of the basal and inducible expression of FABP4, because the expression of *FABP4* in the hepatocytes was nearly 15 times higher than the Kupffer cells isolated from the same mice. The purities of the primary hepatocytes and Kupffer cells were verified by the expression of hepatocyte marker gene albumin (*ALB*) and Kupffer cell marker gene *F4/80*, respectively (Supporting Information Fig. S6). Although the expression of FABP4 in the Kupffer cells is substantially lower than the hepatocytes, we cannot exclude the possibility that Kupffer cells may have also played a role in the phenotypical exhibition. In the liver and besides ASH, inhibition of FABP4 attenuated mice from liver injuries induced by ischemia/reperfusion or sepsis[19,20], whereas adenoviral overexpression of FABP4 sensitized mice to non-alcoholic steatohepatitis[11].

Our results also provide a possible explanation for the contraindication of RIF in alcoholics. RIF is a potent activator of human PXR. Based on our results, we speculate that RIF may have exacerbated ALD by activating PXR and inducing the expression of FABP4 in patients. The implication of PXR in ALD was also supported by several pre-clinical studies. It was reported that both the PXR level and its nuclear translocation were increased upon a long-term ethanol exposure[27]. Our bioinformatic analysis of GSE86002 showed that mice challenged with a 16-week ethanol diet exhibited increased expression of both PXR and CYP3A11 (Supporting Information Fig. S7). In the loss of function models, two recent reports showed that the PXR knockout mice were protected from ALD induced by ethanol diet or acute ethanol exposure, but without defined mechanisms[29,46]. Nevertheless, results from the PXR null mice further supported the sensitizing effect of PXR activation on ALD.

We are aware of the inconsistency of literature regarding the contraindication of RIF in alcoholics. Cross and colleagues concluded that RIF was not contraindicated in patients categorized as alcoholics, but this conclusion was made upon excluding patients with "clinically significant and persistent pretreatment abnormalities of hepatic function tests"[47]. The current drug prescribing information of RIFADIN® still lists alcohol or alcohol abuse as risk factors. Among the limitations of our study, RIF is a human specific PXR agonist, future use of RIF in hPXR humanized mice is necessary to further support that activation of hPXR by RIF sensitizes humanized mice to ASH.

Another clinical significance of our study is the establishment of the PXR−FABP4 regulatory axis as a therapeutic target of ASH. Based on our results, we proposed that PXR-mediated induction of FABP4 represents a feedforward mechanism to exacerbate ALD. This notion was experimentally supported by our observation that the PXR and FABP4 dual inhibitor AG effectively protected mice from ASH. It was noted that AG was reported to improve the chronic alcoholic liver disease by inhibiting NF-κB/TNF-α activation and decreasing ROS levels[48]. Therefore, we cannot exclude the possibility that the effect of AG on NF-κB/TNF-α activation and ROS production contributed to the phenotypic exhibition of our mice. Besides PXR, the transcription of FABP4 is also subjected to regulation by other regulators such as HIF1α, PPAR, LXR, AP-1[49-51]. It appears that in the regulation of FABP4, PXR is dominating in the liver, but in other tissues, these other regulators such as HIF1α, PPAR, LXR, AP-1 outperform PXR in regulating FABP4. To support this speculation, we bioinformatically analyzed the expression levels of these factors in multiple tissues from mice (GSE10246). The result show that the

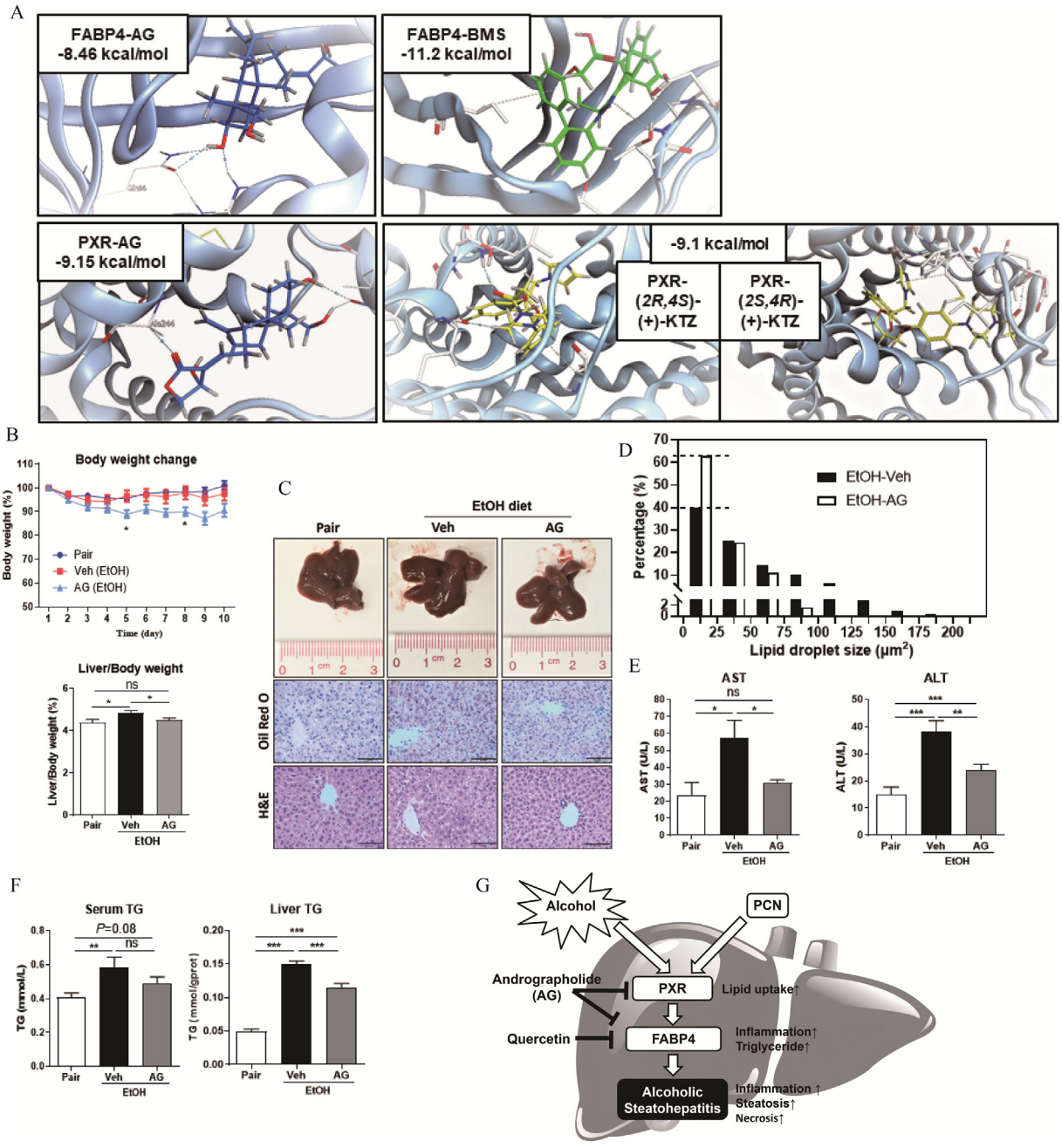

Figure 6 The PXR and FABP4 dual inhibitor andrographolide protects mice from alcoholic steatohepatitis. (A) Molecular docking results of FABP4-AG and PXR-AG bindings, as compared to FABP4-BMS and PXR-KTZ bindings. (B−F) C57BL/6 male mice were subjected to NIAAA model of alcoholic steatohepatitis in the presence of either vehicle (saline) or Andrographolide (50 mg/kg/day) by i.p. injections. Shown are growth curve, liver weight and liver/body weight ratio of mice (B), histological analysis of mice liver samples (scale bar: 50 μm) (C), distribution of lipid droplet sizes (D), serum AST and ALT levels (E), and serum and hepatic TG levels (F). (G) Summary of the role of PXR−FABP4 gene regulatory axis in the progression of alcoholic steatohepatitis and how the axis can be pharmacologically inhibited. Data are presented as mean ± SD, $n = 5-6$; $^{*}P < 0.05$, $^{**}P < 0.01$, $^{***}P < 0.001$. ns, statistically not significant.

mRNA level of PXR (NR1I2) was predominant in liver, comparing with the other tissues such as WAT, BAT, lung, and kidney. LXRα (NR1H3) is also highly expressed in the liver. In contrast, the relative expression of PPARγ, JUN (c-Jun, most extensively studied protein of the AP-1 complex) and HIF1A was much less prominent in the liver (data hot shown). Also, in addition to inhibiting one of the upstream transcriptional regulators, another potential therapeutic approach is direct inhibition of FABP4, but the relative effectiveness of these two approaches remains to be experimentally investigated.

5. Conclusions

In summary, we have uncovered a novel function of PXR activation in sensitizing rodents and likely human patients to ASH. The PXR−FABP4 regulatory axis may represent a novel

therapeutic target and agents targeting PXR and FABP4 individually or in combination may have their promise in the clinical management of alcoholic steatohepatitis.

Acknowledgments

This work was supported by the National Natural Science Foundation of China (Grant Nos. 82020108031, 82404752, 81730103, 81573507 and 81973398), The National Key Research and Development Program (Grant Nos. 2017YFC0909300 and 2016YFC0905000, China), Guangdong Provincial Key Laboratory of Construction Foundation (Grant Nos. 2017B030314030 and 2020B1212060034, China), Science and Technology Program of Guangzhou (Grant No. 201607020031, China), National Engineering and Technology Research Center for New drug Druggability Evaluation (Seed Program of Guangdong Province (Grant No. 2017B090903004, China), the 111 project (Grant No. B16047, China), Guangdong Basic and Applied Basic Research Foundation (Grant Nos. 2022A1515012549 and 2023A1515012667, China), and Marine Medicine Innovation Platform for the Integration of Production and Education Project of Guangdong Provincial Education Department (No. 2021CJPT014, China), Shenzhen Stability Support Project for Colleges and Universities (No. 20220814205518001, China) and Shenzhen Sustainable Development Project (No. KCXFZ20230731094501002, China).

Author contributions

Yiwen Zhang: Data curation. Bingfang Hu: Writing − review & editing, Writing − original draft, Conceptualization. Shaoxing Guan: Writing − review & editing, Writing − original draft, Funding acquisition, Data curation. Pan Li: Writing − review & editing, Visualization, Software. Yingjie Guo: Methodology. Pengfei Xu: Methodology. Yongdong Niu: Methodology. Yujin Li: Methodology. Ye Feng: Methodology, Investigation. Jiewen Du: Visualization, Software. Jun Xu: Visualization, Software. Xiuchen Guan: Methodology. Jingkai Gu: Writing − review & editing. Haiyan Sun: Writing − review & editing, Writing − original draft, Funding acquisition. Min Huang: Writing − review & editing, Writing − original draft, Funding acquisition, Conceptualization.

Conflicts of interest

The authors declare no competing interests.

Appendix A. Supporting information

Supporting information to this article can be found online at https://doi.org/10.1016/j.apsb.2024.08.029.

References

1. O'Shea RS, Dasarathy S, McCullough AJ. Alcoholic liver disease. *Hepatology* 2010;**51**:307−28.
2. Suk KT, Kim MY, Baik SK. Alcoholic liver disease: treatment. *World J Gastroenterol* 2014;**20**:12934−44.
3. Mandayam S, Jamal MM, Morgan TR. Epidemiology of alcoholic liver disease. *Semin Liver Dis* 2004;**24**:217−32.
4. Marrero JA, Fontana RJ, Fu S, Conjeevaram HS, Su GL, Lok AS. Alcohol, tobacco and obesity are synergistic risk factors for hepatocellular carcinoma. *J Hepatol* 2005;**42**:218−24.
5. Testino G, Leone S, Borro P. Alcohol and hepatocellular carcinoma: a review and a point of view. *World J Gastroenterol* 2014;**20**:15943−54.
6. Gao B, Bataller R. Alcoholic liver disease: pathogenesis and new therapeutic targets. *Gastroenterology* 2011;**141**:1572−85.
7. Che Z, Song Y, Xu C, Li W, Dong Z, Wang C, et al. Melatonin alleviates alcoholic liver disease *via* EGFR−BRG1−TERT axis regulation. *Acta Pharm Sin B* 2023;**13**:100−12.
8. Wang W, Liu P, Zhang Y, Yan L, Zhu MX, Wang J, et al. Expression and functions of transient receptor potential channels in liver diseases. *Acta Pharm Sin B* 2023;**13**:445−59.
9. Kazemi MR, McDonald CM, Shigenaga JK, Grunfeld C, Feingold KR. Adipocyte fatty acid-binding protein expression and lipid accumulation are increased during activation of murine macrophages by toll-like receptor agonists. *Arterioscler Thromb Vasc Biol* 2005;**25**:1220−4.
10. Boord JB, Maeda K, Makowski L, Babaev VR, Fazio S, Linton MF, et al. Combined adipocyte-macrophage fatty acid-binding protein deficiency improves metabolism, atherosclerosis, and survival in apolipoprotein E-deficient mice. *Circulation* 2004;**110**:1492−8.
11. Hoo RL, Lee IP, Zhou M, Wong JY, Hui X, Xu A, et al. Pharmacological inhibition of adipocyte fatty acid binding protein alleviates both acute liver injury and non-alcoholic steatohepatitis in mice. *J Hepatol* 2013;**58**:358−64.
12. Hotamisligil GS, Johnson RS, Distel RJ, Ellis R, Papaioannou VE, Spiegelman BM. Uncoupling of obesity from insulin resistance through a targeted mutation in aP2, the adipocyte fatty acid binding protein. *Science* 1996;**274**:1377−9.
13. Furuhashi M, Tuncman G, Görgün CZ, Makowski L, Atsumi G, Vaillancourt E, et al. Treatment of diabetes and atherosclerosis by inhibiting fatty-acid-binding protein aP2. *Nature* 2007;**447**:959−65.
14. Makowski L, Boord JB, Maeda K, Babaev VR, Uysal KT, Morgan MA, et al. Lack of macrophage fatty-acid-binding protein aP2 protects mice deficient in apolipoprotein E against atherosclerosis. *Nat Med* 2001;**7**:699−705.
15. Tang W, Ding Z, Gao H, Yan Q, Liu J, Han Y, et al. Targeting Kindlin-2 in adipocytes increases bone mass through inhibiting FAS/PPARγ/FABP4 signaling in mice. *Acta Pharm Sin B* 2023;**13**:4535−52.
16. Chiyonobu N, Shimada S, Akiyama Y, Mogushi K, Itoh M, Akahoshi K, et al. Fatty acid binding protein 4 (FABP4) overexpression in intratumoral hepatic stellate cells within hepatocellular carcinoma with metabolic risk factors. *Am J Pathol* 2018;**188**:1213−24.
17. Hui X, Li H, Zhou Z, Lam KS, Xiao Y, Wu D, et al. Adipocyte fatty acid-binding protein modulates inflammatory responses in macrophages through a positive feedback loop involving c-Jun NH_2-terminal kinases and activator protein-1. *J Biol Chem* 2010;**285**:10273−80.
18. Makowski L, Brittingham KC, Reynolds JM, Suttles J, Hotamisligil GS. The fatty acid-binding protein, aP2, coordinates macrophage cholesterol trafficking and inflammatory activity. Macrophage expression of aP2 impacts peroxisome proliferator-activated receptor gamma and IkappaB kinase activities. *J Biol Chem* 2005;**280**:12888−95.
19. Hu B, Guo Y, Garbacz WG, Jiang M, Xu M, Huang H, et al. Fatty acid binding protein-4 (FABP4) is a hypoxia inducible gene that sensitizes mice to liver ischemia/reperfusion injury. *J Hepatol* 2015;**63**:855−62.
20. Hu B, Li Y, Gao L, Guo Y, Zhang Y, Chai X, et al. Hepatic induction of fatty acid binding protein 4 plays a pathogenic role in sepsis in mice. *Am J Pathol* 2017;**187**:1059−67.
21. Kliewer SA, Moore JT, Wade L, Staudinger JL, Watson MA, Jones SA, et al. An orphan nuclear receptor activated by pregnanes defines a novel steroid signaling pathway. *Cell* 1998;**92**:73−82.
22. Lei S, Guo A, Lu J, Qi Q, Devanathan AS, Zhu J, et al. Activation of PXR causes drug interactions with Paxlovid in transgenic mice. *Acta Pharm Sin B* 2023;**13**:4502−10.
23. Zhou J, Zhai Y, Mu Y, Gong H, Uppal H, Toma D, et al. A novel pregnane X receptor-mediated and sterol regulatory element-binding protein-independent lipogenic pathway. *J Biol Chem* 2006;**281**:15013−20.

24. He J, Gao J, Xu M, Ren S, Stefanovic-Racic M, O'Doherty RM, et al. PXR ablation alleviates diet-induced and genetic obesity and insulin resistance in mice. *Diabetes* 2013;**62**:1876−87.
25. Zhou J, Febbraio M, Wada T, Zhai Y, Kuruba R, He J, et al. Hepatic fatty acid transporter Cd36 is a common target of LXR, PXR, and PPARgamma in promoting steatosis. *Gastroenterology* 2008;**134**:556−67.
26. Zhang J, Wei Y, Hu B, Huang M, Xie W, Zhai Y. Activation of human stearoyl-coenzyme A desaturase 1 contributes to the lipogenic effect of PXR in HepG2 cells. *PLoS One* 2013;**8**:e67959.
27. Je YT, Sim WC, Kim DG, Jung BH, Shin HS, Lee BH. Expression of CYP3A in chronic ethanol-fed mice is mediated by endogenous pregnane X receptor ligands formed by enhanced cholesterol metabolism. *Arch Toxicol* 2015;**89**:579−89.
28. Thompson JE. The effect of rifampicin on liver morphology in tuberculous alcoholics. *Aust N Z J Med* 1976;**6**:111−6.
29. Choi S, Neequaye P, French SW, Gonzalez FJ, Gyamfi MA. Pregnane X receptor promotes ethanol-induced hepatosteatosis in mice. *J Biol Chem* 2018;**293**:1−17.
30. Guo W, Liu W, Chen G, Hong S, Qian C, Xie N, et al. Water-soluble andrographolide sulfonate exerts anti-sepsis action in mice through down-regulating p38 MAPK, STAT3 and NF-κB pathways. *Int Immunopharmacol* 2012;**14**:613−9.
31. Islam MT. Andrographolide, a new hope in the prevention and treatment of metabolic syndrome. *Front Pharmacol* 2017;**8**:571.
32. Wang Y, Wei B, Wang D, Wu J, Gao J, Zhong H, et al. DNA damage repair promotion in colonic epithelial cells by andrographolide downregulated cGAS−STING pathway activation and contributed to the relief of CPT-11-induced intestinal mucositis. *Acta Pharm Sin B* 2022;**12**:262−73.
33. Yan H, Huang Z, Bai Q, Sheng Y, Hao Z, Wang Z, et al. Natural product andrographolide alleviated APAP-induced liver fibrosis by activating Nrf2 antioxidant pathway. *Toxicology* 2018;**396**−**397**:1−12.
34. Wang Y, Hu JS, Lin HQ, Ip TM, Wan DC. Herbalog: a tool for target-based identification of herbal drug efficacy through molecular docking. *Phytomedicine* 2016;**23**:1469−74.
35. Ooi JP, Kuroyanagi M, Sulaiman SF, Muhammad TS, Tan ML. Andrographolide and 14-deoxy-11,12-didehydroandrographolide inhibit cytochrome P450s in HepG2 hepatoma cells. *Life Sci* 2011;**88**:447−54.
36. Bertola A, Mathews S, Ki SH, Wang H, Gao B. Mouse model of chronic and binge ethanol feeding (the NIAAA model). *Nat Protoc* 2013;**8**:627−37.
37. Xie W, Barwick JL, Simon CM, Pierce AM, Safe S, Blumberg B, et al. Reciprocal activation of xenobiotic response genes by nuclear receptors SXR/PXR and CAR. *Genes Dev* 2000;**14**:3014−23.
38. Kirpich I, Ghare S, Zhang J, Gobejishvili L, Kharebava G, Barve SJ, et al. Binge alcohol-induced microvesicular liver steatosis and injury are associated with down-regulation of hepatic Hdac 1, 7, 9, 10, 11 and up-regulation of Hdac 3. *Alcohol Clin Exp Res* 2012;**36**:1578−86.
39. Roychowdhury S, Chiang DJ, Mandal P, McMullen MR, Liu X, Cohen JI, et al. Inhibition of apoptosis protects mice from ethanol-mediated acceleration of early markers of CCl_4-induced fibrosis but not steatosis or inflammation. *Alcohol Clin Exp Res* 2012;**36**:1139−47.
40. Kittayaruksakul S, Zhao W, Xu M, Ren S, Lu J, Wang J, et al. Identification of three novel natural product compounds that activate PXR and CAR and inhibit inflammation. *Pharm Res (N Y)* 2013;**30**:2199−208.
41. Teixeira TS, Freitas RF, Abrahão Jr O, Devienne KF, de Souza LR, Blaber SI, et al. Biological evaluation and docking studies of natural isocoumarins as inhibitors for human kallikrein 5 and 7. *Bioorg Med Chem Lett* 2011;**21**:6112−5.
42. Szklarczyk D, Gable AL, Nastou KC, Lyon D, Kirsch R, Pyysalo S, et al. The STRING database in 2021: customizable protein−protein networks, and functional characterization of user-uploaded gene/measurement sets. *Nucleic Acids Res* 2021;**49**:D605−12.
43. Xie W, Barwick JL, Downes M, Blumberg B, Simon CM, Nelson MC, et al. Humanized xenobiotic response in mice expressing nuclear receptor SXR. *Nature* 2000;**406**:435−9.
44. Cui JY, Gunewardena SS, Rockwell CE, Klaassen CD. ChIPing the cistrome of PXR in mouse liver. *Nucleic Acids Res* 2010;**38**:7943−63.
45. Ding L, Li J, Song B, Xiao X, Huang W, Zhang B, et al. Andrographolide prevents high-fat diet-induced obesity in C57BL/6 mice by suppressing the sterol regulatory element-binding protein pathway. *J Pharmacol Exp Ther* 2014;**351**:474−83.
46. Choi S, Gyamfi AA, Neequaye P, Addo S, Gonzalez FJ, Gyamfi MA. Role of the pregnane X receptor in binge ethanol-induced steatosis and hepatotoxicity. *J Pharmacol Exp Ther* 2018;**365**:165−78.
47. Cross FS, Long MW, Banner AS, Snider Jr DE. Rifampin-isoniazid therapy of alcoholic and nonalcoholic tuberculous patients in a U.S. Public healthservice cooperative therapy trial. *Am Rev Respir Dis* 1980;**122**:349−53.
48. Song Y, Wu X, Yang D, Fang F, Meng L, Liu Y, et al. Protective effect of andrographolide on alleviating chronic alcoholic liver disease in mice by inhibiting nuclear factor κ B and tumor necrosis factor alpha activation. *J Med Food* 2020;**23**:409−15.
49. Lee YS, Kim JY, Oh KS, Chung SW. Fatty acid-binding protein 4 regulates fatty infiltration after rotator cuff tear by hypoxia-inducible factor 1 in mice. *J Cachexia Sarcopenia Muscle* 2017;**8**:839−50.
50. Laouirem S, Sannier A, Norkowski E, Cauchy F, Doblas S, Rautou PE, et al. Endothelial fatty liver binding protein 4: a new targetable mediator in hepatocellular carcinoma related to metabolic syndrome. *Oncogene* 2019;**38**:3033−46.
51. Tang Z, Shen Q, Xie H, Zhou X, Li J, Feng J, et al. Elevated expression of FABP3 and FABP4 cooperatively correlates with poor prognosis in non-small cell lung cancer (NSCLC). *Oncotarget* 2016;**7**:46253−62.